Social behavior–induced multistability in minimal competitive ecosystems

Article *in* Journal of Theoretical Biology · November 2017

DOI: 10.1016/j.jtbi.2017.11.016

CITATIONS
4

READS
202

Social behavior-induced multistability in minimal competitive ecosystems

D. Melchionda[†], E. Pastacaldi[†], C. Perri[†], M. Banerjee[‡,*], E. Venturino[†]
[†]Dipartimento di Matematica "Giuseppe Peano" via Carlo Alberto 10, Università di Torino, 10123 Torino, Italy
[‡]Department of Mathematics & Statistics, IIT Kanpur, India

Abstract

Mimimal models of coordinated behavior of populations living in the same environment are introduced for the cases when they either both gain by mutual interactions, or one hunts the other one, or finally when they compete with each other. The equilibria of the systems are analysed, showing that in some cases the populations may both disappear. Coexistence leads to global asymptotic stability for symbiotic populations, or to Hopf bifurcations for predator-prey systems. Finally, a new very interesting phenomenon is discovered in the competition case: tristability may be achieved showing that the principle of competitive exclusion fails in this case. Indeed either one of the competing populations may thrive, but also the case of populations coexistence is allowed, for the same set of parameter values.

Keywords: predator-prey; symbiosis; competitive exclusion; group gathering; tristability; ecosystems.
AMS subject classification: 92D25, 92D40

1 Introduction

In the almost one-century-long history of mathematical modeling of population interactions, mostly their individualistic behavior has been taken into account. Only relatively recently the effect of group defense has been explicitly modeled, [15]. A slightly different concept is herd behavior, introduced in [1]. In this paper we extend it to encompass more general situations. We consider minimal models for two populations whose intermingling may be beneficial to both of them, beneficial for one and detrimental for the other one, or harmful for both of them. The classical models always assume individualistic behavior of each population, see e.g. Part I of [24]. Here, we remove this assumption by rather using the recently introduced concepts for mimicking the herd

*Corresponding author. E-mail: malayb@iitk.ac.in

group gathering of herbivores. In fact new models of such type have been considered in [1] and in several other following papers e.g. [3, 4, 5, 23]. These differ quite a bit from other earlier ideas relying on different assumptions on the shape of the functional response, [15], or from more recent contributions, [16], in which starting from first principles and using the Becker and Döring equations for group size dynamics, a functional response similar to Holling type II (HTII) is derived for the predators, although individuals follow a Holling type I (HTI) dynamics. The biological literature abounds on social, herd or pack behaviour, using concepts modeled via different mathematical tools, e.g. graph theory or game theory, see for instance [17, 31] and the wealth of literature that is cited in these papers. In the framework of animals' socialized behavior these ideas have recently been discussed also in [3] and carried over to ecoepidemic systems in which the disease affects the predators, [18], or considering several possibilities for the infected prey, that they may remain in the herd or be left behind, [8, 22].

In this paper we confine ourselves only to the pure demographic situation, i.e. to models in the absence of the disease. The basic picture is herbivores that gather in a herd and wander grazing grass, assumed to be always available; when it becomes scarce, the herd moves to more favorable pastures. When predators are considered, we assume them also to gather in a pack, follow the herbivores and hunt them in a coordinate fashion. At the individual level, each individual competes with its similars for space, as the resource is assumed, as said above, always available. Thus, the logistic form for the population growth is a suitable assumption. At the population level, the interaction is assumed to occur, again on a one-to-one basis, only among the individuals in the two populations that occupy the outermost positions in each group. This is the basic distinctive feature of the models introduced in this paper, with respect to [1, 8, 18, 33]. In these former studies, in fact, only one of the two interacting populations gathers in a herd, while the other one behaves individualistically.

We consider two populations, each forming a group, that interact in various ways. In particular, for the predator-prey case, when the predators' pack hunts the prey some individuals generally have a larger benefit. They are those that either take the best (social) positions because they are stronger and therefore attack the prey before the other ones, obtaining a better gain, or simply those that get the most advantageous (spatial) positions in the community in order to get the best share of the prey. We assume therefore that in such case positions on the boundary of the pack have the best returns for the individuals that occupy them, since they are the first to fall upon the prey. The main idea of community behaviors for predators had been considered in [12]. Various forms of functional responses are derived corresponding to different assumptions in the hunting behavior, e.g. a ratio-dependent response function is obtained when predators are localized, i.e. the geometry of the pack is not changed by adding more predators to it. On the other hand, the Hassell-Varley function, [21], is obtained if the prey are captured in proportion to the area swept by the pack, which depends on its front section.

In the present investigation, when a predator-prey interaction is considered, we examine two situations for the prey, namely when they behave individualistically or when they gather in herds, following the assumptions of [1]. In the latter situation, the most harmed prey during predators' hunting are those staying on the boundary of the herd.

Here however we also extend the concept of group gathering to more general types of interac-

tions among populations thriving in the same environment. The cases of symbiosis and competition are also well-known in the literature, for the Lotka-Volterra competition system in particular see [34]. Again, the classical approach, in which both populations behave individualistically, will be replaced by more social attitudes, such as herd or pack behavior. In part this idea has been introduced in [1], but assuming that only one population behaves socially, the individuals of the other one live independently of each other. Thus, we extend now the analysis to the case in which both populations show a community behavior, both when each one of the two communities benefits from the interactions with the other one, as well as to the case in which the communities compete with each other. More specific ecological examples will be discussed below.

The systems introduced here are intended to be minimal, in order to emphasize their outcomes due to the specific herd behavior assumptions made. In this idealized setting, the interactions occurring on the edge of the pack are mathematically modeled via suitable nonlinear functions of the populations. These nonlinearities are purposely chosen to replace the classical terms coming from the mass action law, containing products of the two populations. These nonlinearities represented by Gompertz-like interaction terms, i.e. terms in which the populations appear raised to a fixed exponent, whose value is $\frac{1}{2}$. This value comes from its geometric meaning, it represents the fact that the perimeter of the patch occupied by the population is one-dimensional, while the patch itself is two-dimensional, as explained in detail below.

The basic ideas underlying modeling herd behavior have been expounded in [1]. For the benefit of the reader we recall here the main steps. Consider a population that gathers together. Let P represent its size. If this population occupies a certain territory of size A, the number of individuals staying at the outskirts of the group, be it the pack or the herd, is directly related to the length of the perimeter of the territory occupied by the herd. Therefore its length is proportional to $\sqrt{A}$. We take the population P to be homogeneously distributed over the two-dimensional domain A. Thus its square root, i.e. $\sqrt{P}$ will count the individuals on the perimeter of the territory.

Let us assume that another population Q intermingles with the one just considered. At first, assume that Q behaves individualistically, the individuals do not gather in a group. We assume that the interactions of the latter with the former population occur mainly via the individuals in it living at the periphery, which are proportional to $\sqrt{P}$, as mentioned. Thus the interaction terms in this case are proportional to $Q\sqrt{P}$.

Instead let us now assume that the second population Q gathers in a group and intermingles with P. Assuming again that the interactions of the two populations occur mainly via the individuals living at the periphery, in this case the interaction terms must be proportional to the subsets of the two populations on the edge of their respective groups and therefore will contain square root terms for both populations. They will thus be modeled via $\sqrt{Q}\sqrt{P}$.

Further, interactions between population can be of different types. They can benefit both, in the case of symbiosis. Alternatively they can damage both populations, when they compete among themselves directly or for common resources. Finally, one population receives an advantage at the expense of the other one; this happens in the predator-prey situation. As a consequence, note that these mathematical differences involve sign changes in the corresponding interaction terms. With the exception that involves pack predation and individual prey, not considered in [1], we will concentrate on models involving both populations with individuals sticking together. In the models

under scrutiny in this paper, we keep the biological setting to a minimum, in order to highlight the differences that this formulation entails with respect to the classical one-to-one interaction models.

To better ecologically motivate the models, we illustrate here some possible biological examples for each envisaged situation.

For the predator-prey case a simple example of the two possible demographic interactions is provided by wolves (*Canis lupus*) or other carnivores hunting in packs either isolated prey or herds of herbivores.

The symbiotic case can be illustrated in several ways. There are several associations between populations that are beneficial to both, or beneficial to one and neutral for the other one. For instance, in the roots of legumes, diverse microbiomes, rhizobia, nitrogen-fixing bacteria are found, while in alder root nodules thrive actinomycete nitrogen-fixing Frankia bacteria, [27], [29] p. 142, so that, mainly producing malate and succinate dicarboxylic acids, photosynthesis can occur. Fungi can penetrate the cortex cells of the plant's secondary roots, thereby forming an association named mycorrhiza. Most of land ecosystems depend on the beneficial associations between mycorrhyzal fungi, that extract minerals, inorganic nitrogen and phosphorus, from the ground and the plants, fixing carbon from the air, [20]. The fungi may also secrete antibiotics thereby protecting the host plant from parasitic fungi and bacteria. It is well known, [30], that symbiotic relationships among fungi in arbuscular mycorrhizas involve about 80% of the plants. Note that we mention this example in spite of the fact that it represents a three-dimensional structure. It therefore would require a modification of the square root term in our model, which would become the power $2/3$. Indeed this is the ratio of surface area to volume in a three-dimensional situation and would replace the ratio perimeter to area of the two-dimensional case. In a very recent investigation, this problem has been addressed in its full generality, [6], allowing for a general exponent α encompassing also possible fractal domains. Although we could also consider the general situation in this paper, however, we prefer to address the square root situation only, to better illustrate the ecological implications without obscuring them with more complicated mathematics.

Another instance of association beneficial to both populations is provided by bullhorn acacia trees harboring stinging ants among their thorns. The acacia tree provides the ants with food, its very sweet nectar exhudating from nectaries, its specialized structures, and the Beltian bodies, food nodules growing on the leaves. Ants in turn attack anything approaching the perimeter of their host, even killing branches of neighboring trees and removing all the vegetation around their tree's trunk. Epiphytes, like orchids and other members of the pineapple family, thrive on the edge of stronger plants gaining better sunlight exposure, but do not assume nourishment from their host.

In the marine world finally, the mollusc *Elysia viridis* (Mollusca) hosts the endosymbiont *Codium fragile*, that produces Photosynthates, while obtaining protection and inorganic nutrients, [32].

In all these examples, note that the interactions occur on the perimeter of the occupied areas of each population, or through the surface of their leaves or roots. It makes therefore sense to investigate these population interactions via square root terms as explained above.

For the case of competing populations, an example of this situation is provided by herbivores sharing, or better, competing, for grass in high pastures. In the Alps, during the summer season domestic animals like goats and cows are brought into the high pastures for feeding. These herds

become in close contact, but do not intermingle, with the wild herds of chamoises (*Rupicapra r. rupicapra*) and ibexes (*Capra i. ibex*). Thus the interactions among domestic goats and cows with wild herbivores, occurring at the edge of the respective herds, has negative consequences for both, as food is subtracted from one population to the other one, and vice versa. Note that the interactions are really close, so that even diseases like infectious keratoconjunctivitis can be transmitted from one herd to the other one, [25].

The paper is organized as follows. The next Section presents the two predator-prey cases. Section 3 investigates the cases of symbiosis. Section 4 presents the competing populations, showing new unexpected results with respect to the corresponding classical case. A final discussion concludes the paper, comparing these findings with the classical models. The appendix contains the mathematical preliminaries, the analysis of the system's equilibria and the investigation also of the more complex behavior of these models.

To sum up, the novelty of this work lies in the study of predators' pack hunting of either individual or herd-gathered prey, Both minimal models introduced in Section 2 are therefore new, in view of the presence of the square root terms for the predators. For the symbiotic and competing cases, again the models are new because they contain square root terms for both interaction terms. The findings indicate an unexpected outcome for the competition, namely tristability, which is impossible for the classical case of 1-1 interactions among competing populations. This results shows that the principle of competitive exclusion may not hold under these "peripheral interactions" assumptions.

2 The predator-prey cases

In this section, we let $P(t)$ represent the predators and $Q(t)$ denote the prey populations as functions of time t. There are two possible different situations that can arise, when predators hunt in a coordinate fashion: the prey can either wander about in an isolated fashion, or can gather together in herds.

In the two models that follow, the parameters bear the following meaning. The parameter r is the net growth rate of the Q population, with K being its environment's carrying capacity. The hunting rate on the prey is denoted by the parameter q, while p denotes its reward for the predators and m is their natural death rate. The following systems will be considered, in which all the parameters are assumed to be nonnegative.

First, the predator-prey interactions of pack–individualistic type, for a specialized predator

$$\frac{dQ}{dt} = r\left(1 - \frac{Q}{K}\right)Q - q\sqrt{P}Q, \quad \frac{dP}{dt} = -mP + p\sqrt{P}Q. \tag{2.1}$$

Secondly, the pack predation–herd behavior, system, for a specialized predator

$$\frac{dQ}{dt} = r\left(1 - \frac{Q}{K}\right)Q - q\sqrt{P}\sqrt{Q}, \quad \frac{dP}{dt} = -mP + p\sqrt{P}\sqrt{Q}. \tag{2.2}$$

Corresponding models for the case of generalist predators could be formulated, but are not considered here to reduce the length of the paper.

If one of the two populations disappears the system reduces to one equation. In this circumstance if the prey survive, they follow a logistic growth toward their carrying capacity, while if they vanish, the predators cannot survive. In fact when $Q = 0$ the equation for the predators shows that they exponentially decay to zero. This makes sense biologically, since these are specialistic predators. Thus in these two models the disappearance of both populations is a possibility. The equilibrium corresponding to population's collapse is the origin. Its stability can be analysed by a simple expansion of the governing equations near zero, keeping only the dominant terms.

The predator-prey case (2.1) leads to

$$\frac{dQ}{dt} \sim rQ > 0, \quad \frac{dP}{dt} \sim -mP < 0,$$

so that the origin is unstable. In the case (2.2) instead we find

$$\frac{dQ}{dt} \sim \sqrt{Q}(r\sqrt{Q} - q\sqrt{P}), \quad \frac{dP}{dt} \sim \sqrt{P}(-m\sqrt{P} + p\sqrt{Q})$$

and both populations under unfavorable circumstances may well disappear. This happens when

$$\frac{\sqrt{Q}}{\sqrt{P}} < \min\left\{\frac{m}{p}, \frac{q}{r}\right\}. \tag{2.3}$$

2.1 Pack predation and individualistic prey behavior

We consider now (2.1). The following results hold. Their mathematical proofs are found in Appendix **A1.1**. All positive solutions of (2.1) are forward bounded. Here the coexistence equilibrium $E_2^{[pi]}$ can be evaluated explicitly,

$$E_2^{[pi]} = \left(\frac{rmK}{rm + pqK}, \frac{r^2p^2K^2}{(rm + pqK)^2}\right), \tag{2.4}$$

is clearly always feasible and it is always locally asymptotically stable. Moreover, no persistent oscillatory behavior is allowed and as a further consequence the coexistence equilibrium must also be globally asymptotically stable. In summary, for strictly positive initial conditions, the ecosystem populations evolve necessarily to the values given by the coordinates of $E_2^{[pi]}$, independently of the state of the system that is considered as a starting value.

2.2 Pack predation and prey herd behavior

We focus now on (2.2), please refer to Appendix **A1.2** for more details. Once again, also in this case all positive solutions of (2.2) are forward bounded.

The coexistence equilibrium $E_2^{[ph]}$ has the following analytic representation

$$E_2^{[ph]} = \left(\frac{rm - pq}{rm}K, \frac{rm - pq}{rm^3}Kp^2\right) \tag{2.5}$$

and it is feasible for

$$rm \geq pq. \tag{2.6}$$

When it is unfeasible, the origin is then the only possible equilibrium. Both populations vanish also when (2.6) becomes an equality. This is further asserted by recalling the fact that in the case of (2.2) the origin might indeed be achievable, (2.3). Note that when locally asymptotically stable, the origin is also globally asymptotically stable. In addition, there is a transcritical bifurcation for which $E_2^{[ph]}$ emanates from the equilibrium E_0 when the parameter r raises up to attain the critical value $r^* = pqm^{-1}$.

The coexistence equilibrium of the system (2.2) is locally asymptotically stable if (A.17) holds; in such case we must have

$$r > \max\left\{m, \frac{3pq - m^2}{2m}\right\}.$$

But in the range

$$\frac{pq}{m} < r < \max\left\{m, \frac{3pq - m^2}{2m}\right\}$$

we find that $E_2^{[ph]}$ is unstable. Furthermore, the ecosystem starts oscillating in a persistent manner around the coexistence equilibrium when the bifurcation parameter r crosses the critical value

$$r = r^\dagger = \frac{3pq - m^2}{2m}. \tag{2.7}$$

Figure 1 shows the limit cycles for the dimensionalized model (2.2), letting the simulation run for long times to show that the oscillations are indeed persistent, using the Matlab integration routine ode23t.

Finally, it is worthy to note an interesting phenomenon that hardly occurs in population models, that has already been remarked in [33, 18], namely the fact that the system (2.2) admits trajectories for which the prey go to extinction in finite time, if the initial conditions lie in the set

$$\Xi = \left\{(Q, P) : P > 0, 1 \geq Q \geq \exp\left(-\frac{q}{r}\sqrt{P}\right)\right\}, \tag{2.8}$$

We summarize the equilibria of system (2.2) in the following table.

Parameter conditions	E_0	$E_2^{[ph]}$	Bifurcation
$r < \min\left\{m, \frac{pq}{m}\right\}$	stable	unfeasible	
$r < m, \quad r^* = \frac{pq}{m}$			transcritical
$r > \max\left\{m, \frac{3pq - m^2}{2m}\right\}$	unstable	stable	
$r > m, \quad r = r^\dagger = \frac{3pq - m^2}{2m}$			Hopf
$r > m \quad \frac{pq}{m} < r < \frac{3pq - m^2}{2m}$	unstable	unstable	
$r > m \quad \frac{3pq - m^2}{2m} > r$	unstable	unfeasible	

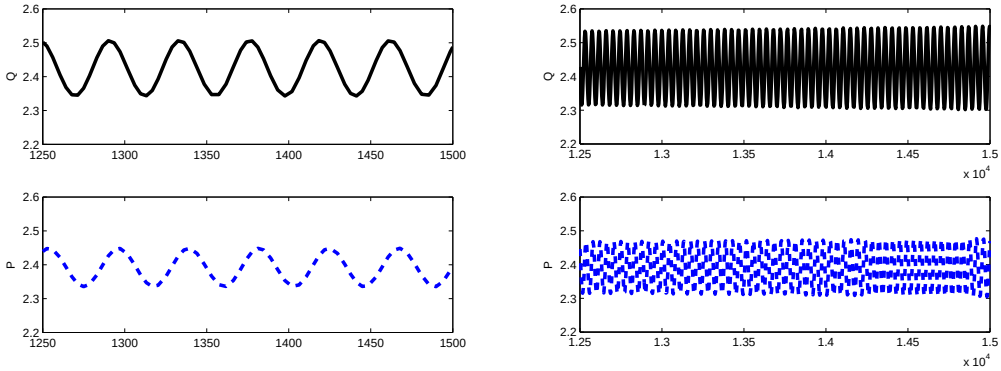

Figure 1: Left: time series of the system trajectories (2.2) up to $t = 1500$; Right: the same situation, but followed for a much longer time, up to $t = 15000$, to show that these are really persistent oscillations. The original parameter values are $r = 0.75937$, $m = 0.299$, $p = 0.297$, $q = 0.61$, $K = 12$; The initial condition is $(2.44, 2.36)$, with coexistence equilibrium $E_2^{[ph]} = (2.4253, 2.3930)$. With these values we obtain $e = 1.2698$ and $f = 0.5066$ so that we are above the dashed line, $e - 2f = 0.2566 > 0$ (coexistence feasibility), but below the continuous line, $0.25 + e - 3f = -1.605 \times 10^{-5} < 0$ (coexistence instability). The eigenvalues of the Jacobian at equilibrium, $0.48 \times 10^{-6} \pm 0.1515\ i$, with positive real part, and the trace of the Jacobian $9.6 \times 10^{-6} > 0$, also positive, both show instability.

3 The symbiotic model

For the mathematical details of this section, please refer to Appendix **A2**. Let us denote by $P(t)$ and $Q(t)$ the sizes of two populations in consideration as functions of time t. The parameters r

and m are the growth rates respectively of the Q and P populations, with K_Q and K_P denoting their carrying capacities. Beneficial interaction rates between the two populations are denoted by the parameter q for the Q population and by p for the P's. The following symbiotic system is considered, in which all the parameters are assumed to be nonnegative:

$$\frac{dQ}{dt} = r\left(1 - \frac{Q}{K_Q}\right)Q + q\sqrt{P}\sqrt{Q}, \quad \frac{dP}{dt} = m\left(1 - \frac{P}{K_P}\right)P + p\sqrt{P}\sqrt{Q}. \tag{3.1}$$

If one of the two populations disappears the system reduces to one equation and the surviving population tends to its own carrying capacity.

The equilibrium corresponding to both population's collapse is the origin. Its stability can be analysed by a simple expansion of the governing equations near zero, keeping only the dominant terms:

$$\frac{dQ}{dt} \sim \sqrt{Q}(r\sqrt{Q} + q\sqrt{P}) > 0, \quad \frac{dP}{dt} \sim \sqrt{P}(m\sqrt{P} + p\sqrt{Q}) > 0.$$

Thus both symbiotic populations cannot vanish.

The investigation of the coexistence equilibrium E_3^S of both populations shows that it results unconditionally feasible and the system trajectories remain forward bounded. Further, populations cannot exhibit persistent oscillations around this point, as Hopf bifurcations are shown never to arise, and the system trajectories remain forward bounded. These results imply also that the coexistence equilibrium is globally asympotically stable. Summing up these considerations, in this case the ecosystem always evolves toward an equilibrium point at which both populations thrive, this being independent of its initial or present conditions.

4 The competition model

As for the symbiotic model let $P(t)$ and $Q(t)$ denote the populations of interest, r and m their net growth rates, K_Q and K_P their carrying capacities, q and p their competition rates. The competing model, where all the parameters are nonnegative, is

$$\frac{dQ}{dt} = r\left(1 - \frac{Q}{K_Q}\right)Q - q\sqrt{P}\sqrt{Q}, \quad \frac{dP}{dt} = m\left(1 - \frac{P}{K_P}\right)P - p\sqrt{P}\sqrt{Q}. \tag{4.1}$$

First of all, the model is ecologically well-posed in view of the fact that the positive solutions of (4.1) are forward bounded. Again the details are contained in Appendix **A3**.

Again, if one of the two populations disappears the surviving one grows logistically to its own carrying capacity. This ecosystem can also totally disappear, since the stability of the origin can be analysed by a simple expansion of the governing equations near zero, keeping only the dominant terms:

$$\frac{dQ}{dt} \sim \sqrt{Q}(r\sqrt{Q} - q\sqrt{P}), \quad \frac{dP}{dt} \sim \sqrt{P}(m\sqrt{P} - p\sqrt{Q}).$$

In this case both populations may disappear, when

$$\frac{m}{p} < \frac{\sqrt{Q}}{\sqrt{P}} < \frac{q}{r}. \tag{4.2}$$

The coexistence equilibria can be obtained as an intersection of cubic functions, shown in Figure 2. Several outcomes are possible, giving rise in some cases to multiple equilibria. Specifically, if

$$pq > rm \tag{4.3}$$

no feasible coexistence equilibria exist. If

$$pq < rm \tag{4.4}$$

at least one feasible equilibrium exists, $E_3^C = (X_3^C, Y_3^C)$. Further, in such case, three equilibria may exist, i.e. E_4^C, E_3^C and E_5^C, ordered for increasing values of their abscissae. The sufficient conditions ensuring these three equilibria to exist are

$$\frac{m}{p}\frac{2}{3\sqrt{3}} > \frac{\sqrt{K_Q}}{\sqrt{K_P}} > \frac{q}{r}\frac{3\sqrt{3}}{2} \tag{4.5}$$

In addition, the equilibria for which either one of the conditions

$$Q < \frac{K_Q}{3}, \quad P < \frac{K_P}{3}, \tag{4.6}$$

hold are unstable.

Considering Figure 2, in the case of just one equilibrium, it must have at least one coordinate to the left (or below) the one of the local maximum of the function. In the plot, it has the abscissa smaller than the one of the local maximum of the parabola with vertical axis (i.e. the function $Y_{[1]}(X)$ given by (A.24) in Appendix **A3**). Thus when E_3^C is unique, it must be unstable. For the case of three equilibria, evidently E_4^C and E_5^C have either the abscissa (E_4^C) or the height (E_5^C) satisfying the corresponding condition in (4.6). Hence these two equilibria must be unstable as well.

In case of three equilibria, the system exhibits the following additional feature. The equilibrium E_3^C for which both the conditions

$$Q > \frac{K_Q}{3}, \quad P > \frac{K_P}{3}, \tag{4.7}$$

hold is locally asymptotically stable. There is a subcritical pitchfork bifurcation: from the unstable E_3^C three equilibria emanate, with the equilibrium E_3^C becoming stable and the other ones being unstable.

Finally, no persistent oscillations around the coexistence equilibrium can arise.

In Figure 3 we show the behavior of the two populations in the phase plane in each of the three possible cases.

4.1 Bifurcations

In this section we describe the possible local bifurcations that can take place for the appearance and disappearance of interior equilibrium points through two types of local bifurcations, namely

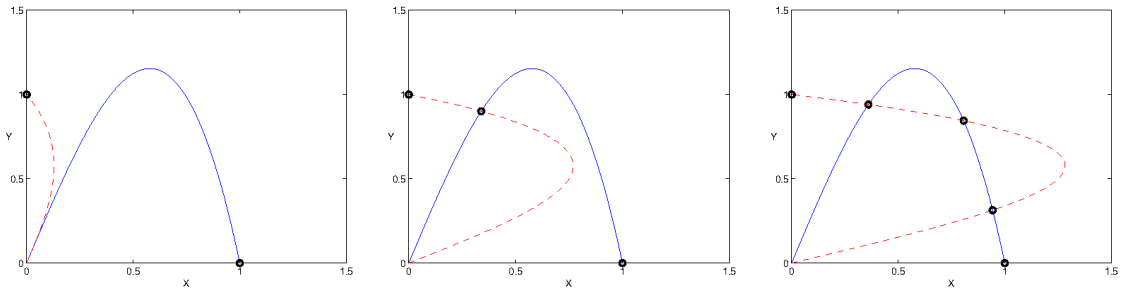

Figure 2: Referring also to Figure 12, we show here the coexistence equilibria possible scenarios. Left: for (4.3) no feasible equilibrium exists for the parameter values $r = 0.9$, $m = 0.3$, $p = 0.9$, $q = 0.3$, $K_p = 10$, $K_q = 10$; the two dots on the axes the two possible system's outcomes, implying the principle of competitive exclusion. Center: (4.5), just one feasible equilibrium E_3^C, for the parameter values $r = 0.9$, $m = 1.8$, $p = 0.9$, $q = 0.3$, $K_p = 10$, $K_q = 10$; Here coexistence is feasible but unstable. Right (4.4) for the parameter values $r = 0.9$, $m = 3$, $p = 0.9$, $q = 0.3$, $K_p = 10$, $K_q = 10$; the three equilibria E_4^C, E_3^C and E_5^C are ordered left to right, for increasing values of their abscissae; E_3, the point in the middle, becomes stable, while the new arising points to its left and right, E_4^C and E_5^C, are unstable. In all the frames, the blue continuous line denotes the population $X(\tau) = \sqrt{Q(t)K_Q^{-1}}$ nullcline, while the red dashed line shows the population $Y(\tau) = \sqrt{P(t)K_P^{-1}}$ nullcline, with variable transformations indicated in the Appendix **A0**.

pitchfork and saddle-node bifurcation. It is important to mention here that the proofs of desired local bifurcations can not be provided with the model (4.1). To prove the fulfilment of the conditions required for the local bifurcations, we thus rather need to consider a transformed model. In what follows we just describe the possible bifurcations, while the detailed proofs of their occurrence are provided at the appendix **A5**.

We investigate first the generation of the interior equilibrium point from the trivial equilibrium point $(0, 0)$ through a pitchfork bifurcation. We consider the model (4.1), fix the parameter values $r = 0.9$; $K_Q = 10$; $q = 0.3$; $K_P = 10$; $p = 0.9$ and let m be the bifurcation parameter. For $m = 0.3$, two non-trivial nullclines of (4.1) are tangent to each other at $(0, 0)$ and we find at least one interior equilibrium point for $m > 0.3$. One interior equilibrium point is generated through a pitchfork bifurcation, another one is not relevant as its components fail to satisfy the feasibility condition. This pitchfork bifurcation threshold is denoted by m_{PF}.

We investigate first the generation of the interior equilibrium point from the trivial equilibrium point $(0, 0)$ through a pitchfork bifurcation. The system (4.1) possesses only one interior equilibrium point for the above mentioned parameter values in the range $m_{PF} < m < 2.059 \equiv m_{SN}$. It has instead three interior equilibrium points, with both components positive, for $m > m_{SN}$. These two new interior equilibrium points are generated through a saddle-node bifurcation at $m = 2.059 \equiv m_{SN}$. For $r = 0.9$, $K_Q = 10$, $q = 0.3$, $K_P = 10$, $p = 0.9$ and $m = 2.059 = m_{SN}$, we find one equilibrium point at $E_1(1.196374618, 8.345124260)$ and two coincident equilibrium

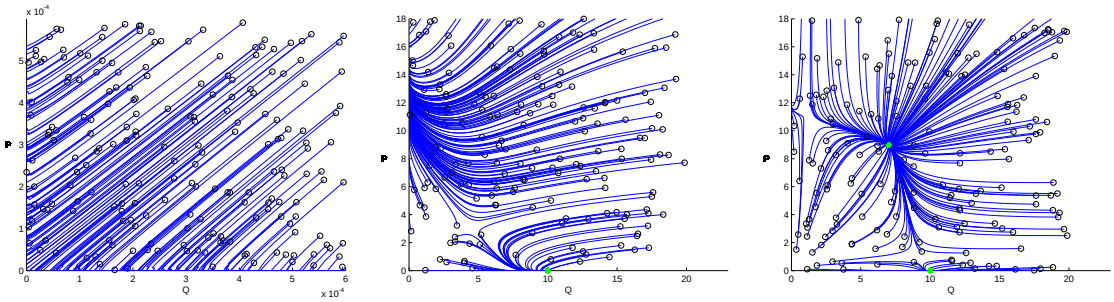

Figure 3: The three possible populations behaviors. Left: the origin is stable, both populations get extinguished; achieved with parameter values $r = 2$, $m = 2$, $p = 33$, $q = 33$, $K_p = 4$, $K_q = 3$ and 200 randomly generated initial conditions, represented by the empty red circles. Note that this occurs also at finite time, when trajectories do not go directly to the origin, but end up on the coordinate axes and then follow them until the origin. Center: bistability and competitive exclusion, only one population survives; achieved with parameter values $r = 0.8888$, $m = 0.602$, $p = 0.401$, $q = 0.5998$, $K_p = 16.5$, $K_q = 10$ and 200 randomly generated initial conditions. Right: tristability, either one population only survives, or the other one, or both together; achieved with parameter values $r = 0.7895$, $m = 0.7885$, $p = 0.225$, $q = 0.2085$, $K_p = 12$, $K_q = 10$ and 200 randomly generated initial conditions. The green full dots, two on the two coordinate axis and one in the first quadrant represent instead the stable equilibria.

points $E_*(7.681094754, 3.717334465)$. The pitchfork and saddle-node bifurcation scenario are shown in Fig. 4 (left).

Depending upon the magnitude of the parameters, we can observe the occurrence of two consecutive saddle-node bifurcations. As a result we obtain one coexisting equilibrium point for two disjoint sets of parameter values and in between we find three interior equilibria. To make this idea more clear, we choose $r = 0.5$; $K_Q = 10$; $q = 0.3$; $K_P = 6$; $p = 0.9$ and let m be the bifurcation parameter as before. Here the relevant thresholds are $m_{PF} = 0.54$, $m_{SN_1} = 2.427$, $m_{SN_2} = 2.7$. We find a unique interior equilibrium point when $m_{PF} < m < m_{SN_1}$ and $c > c_{SN_2}$. Two more interior equilibrium points are generated through the first saddle-node bifurcation threshold at $m = m_{SN_1}$ and again disappear through the second saddle-node bifurcation at $m = m_{SN_2}$. These bifurcation scenarios are presented in Fig. 4 (right).

5 Discussion

5.1 Comparison with the classical cases

5.1.1 The predator-prey ecosystems

In order to compare these results quantitatively, we consider also the classical model with logistic correction. This is needed because if we rescale it, since it does not contain the square root terms,

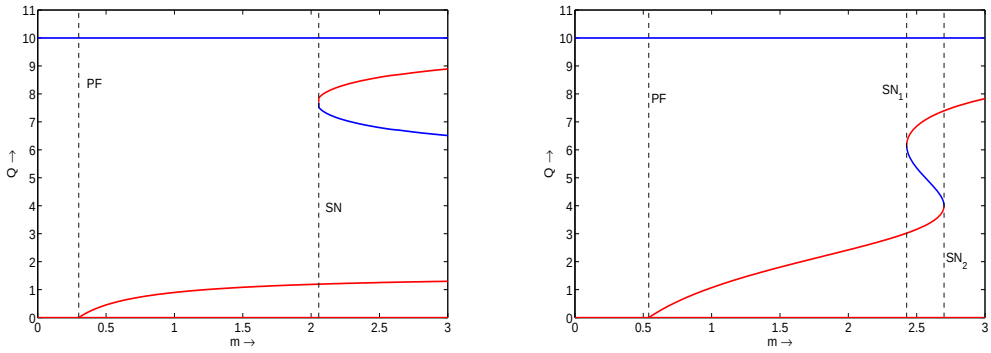

Figure 4: Left: Bifurcation diagram showing the generation of first interior equilibrium point through pitchfork bifurcation followed by the generation of two more interior equilibria through saddle-node bifurcation. Parameter values: $r = 0.9$, $K_Q = 10$, $q = 0.3$, $K_P = 10$, $p = 0.9$. Right: Bifurcation diagram showing the generation of first interior equilibrium point through pitchfork bifurcation followed by the generation and subsequent disappearance of two interior equilibria through two consecutive saddle-node bifurcations. Here the parameter values are $r = 0.5$, $K_Q = 10$, $q = 0.3$, $K_P = 6$, $p = 0.9$.

we would find a different adimensionalization, rendering the comparison difficult. Thus we rather return to the original formulations also for (2.1) and (2.2).

The dimensional form of the coexistence equilibria of the two models (2.1) and (2.2) are (2.4) and (2.5). The dimensional form of the coexistence equilibrium of the classical Lotka-Volterra with logistic correction and of the predator-prey model with individualistic hunting and prey herd behavior, [1], instead are respectively

$$C_* \equiv \left(\frac{m}{p}, \frac{r}{q}\left(1 - \frac{m}{pK}\right)\right), \quad \widetilde{E}_2 = \left(\frac{m^2}{p^2}, \frac{mr}{pq}\left(1 - \frac{m^2}{p^2 K}\right)\right).$$

At these points, the prey equilibrium values depend only on the system parameters m and p, i.e. the predators' mortality and predation efficiency. Thus they are independent of their own reproductive capabilities and of the environment carrying capacity. Further, when the predators' hunting efficiency is larger than the predators' own mortality, i.e. $m < p$, the equilibrium prey value is much lower if they gather in herds, i.e. in $\widetilde{E}_2$, while on the contrary the predators attain instead higher values, again at $\widetilde{E}_2$. Conversely, when $m > p$ the prey grouping together, $\widetilde{E}_2$, allows higher equilibrium numbers than for their individualistic behavior; the predators instead settle at lower values if the prey use a defensive strategy, $\widetilde{E}_2$, and higher ones with individualistic prey behavior, at C_*.

For (2.1) and (2.2), i.e. with coordinated hunting, the equilibrium values involve also the prey own intrinsic characteristics. In particular for (2.2) the ratio of the predators' hunting efficiency p versus the square of their mortality m determines if the predators at equilibrium will be more than the prey, see $E_2^{[ph]}$.

A similar result possibly extends for the model of pack hunting coupled with loose, i.e. individ-

ualistically behaving, prey, (2.1), but at $E_2^{[pi]}$ the predators population at equilibrium contains the prey population squared and in principle the latter may not exceed 1, so that the conclusion would not be immediate. Indeed, at the equilibria $E_2^{[pi]}$ and $E_2^{[ph]}$, the prey populations are the multiplication of the fractions in the brackets, always smaller than 1, by the carrying capacity K, which may or not be large. The result could indeed give a population smaller than 1. This in principle is not a contradiction, because the population need not necessarily be counted by individuals, but rather its size could be measured by the weight of its biomass.

5.1.2 The symbiotic ecosystem

We now try to understand how socialization may possibly boost the mutual benefit of the system's populations.

The symbiotic model has always a stable coexistence equilibrium, while in the classical model the corresponding point $\widehat{E_3^S}$ could be unfeasible, and in such case the trajectories will be unbounded. This is biologically questionable, in view of the limited amount of resources available, However, it shows that in this situation the one-to-one relationship among individuals of different populations may lead to higher benefits for both of them, than the case in which interactions occur only through the marginal areas of contact among them.

Considering instead only parameters choices where $\widehat{E_3^S}$ is feasible, we compare the resulting populations levels for the new and the classical model. Taking for both cases $r = 3$, $m = 3$, $K_Q = 6$, $K_P = 7$, $q = 0.3$, and $p = 0.5$, the behaviors are shown in Figure 5. Starting from the same initial conditions, different equilibria are reached.

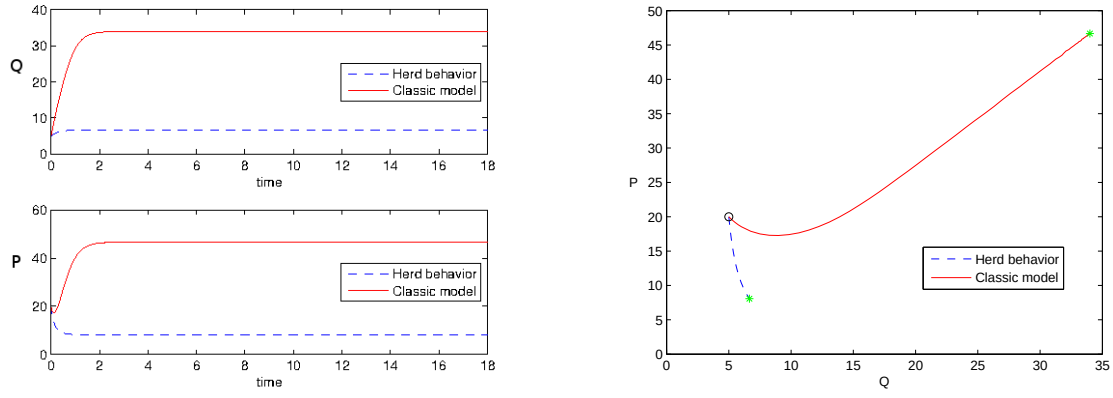

Figure 5: Left: time series of the symbiotic systems (A.19), red continuous, and (3.1), dashed blue, trajectories: top frame Q, bottom frame P; Right: phase plane for classical (A.19) and new (3.1) symbiotic model. Parameter values: $r = 3$, $m = 3$, $K_Q = 6$, $K_P = 7$, $q = 0.3$, and $p = 0.5$. Trajectories originate from the same initial condition $(5, 20)$. The full green dots represent the final equilibrium values.

Clearly the population level is higher in the classical model. The numerical values we obtained are $Q = 6.66$, $P = 8.06$ for the herd model and $Q = 33.99$, $P = 46.69$ for the classical model.

This makes sense, since in symbiotic models the benefit comes from the mutual interactions between populations. If the latter are scattered in the environment it is more likely for each individual of one population to get in contact with one of the other. On the other hand, when herd behaviour is exhibited, only individuals on the outskirts interact with the other population and as a consequence the innermost individuals receive less benefit since they hardly have the chance to meet the other population.

5.1.3 The competition ecosystem

While the classical case exhibits the principle of competitive exclusion, here, instead, we have found that in the presence of community behavior of both populations, the same occurs, but there is another possibility, namely tristability. When the conditions arise, the coexistence equilibrium may be present together with the equilibria in which one population vanishes. Therefore the system's outcome is once more determined by the initial conditions, but this time the phase plane is partitioned into three basins of attractions, corresponding each to one of the possible equilibria. It would be interesting to compute explicitly the boundary of each one of them. For this task state-of-the-art approximation theoretic algorithms have been devised, [9, 10, 11, 13, 14].

We now compare the population levels when a coexistence equilibrium is stable in both classical and new model. Considering the parameters $r = 2$, $m = 3$, $K_Q = 6$, $K_P = 8$, $q = 0.2$ and $p = 0.09$, with suitable initial conditions, the behavior of the two models is shown in Figure 6. From the same initial conditions, trajectories of the two models evolve toward different equilibria. The population levels are thus higher in the herd model, at $Q^C = 6.26$ and $P^C = 9.17$ while for

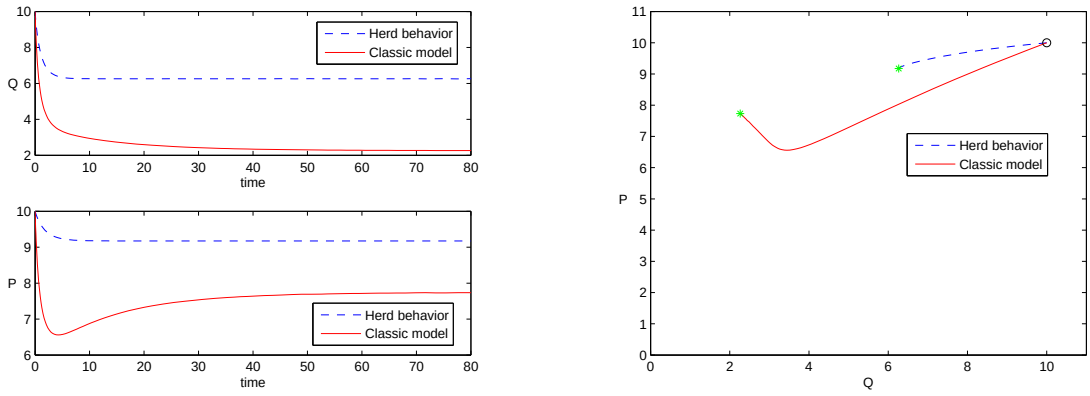

Figure 6: Left: time series of the systems trajectories; Right: phase plane for classical and new competition model. Parameter values: $r = 0.8$, $m = 0.5$, $p = 0.05$, $q = 0.07$, $K_p = 10$, $K_q = 7$. Both trajectories originate from the same initial condition $(10, 10)$. The full green dots represent the equilibrium points.

the classic model we find $\widetilde{Q}^C = 2.26$ and $\widetilde{P}^C = 7.74$. This is not surprising for the same reasons for which the opposite behavior occurs in the symbiotic models. In herd models, only individuals at the outskirts meet individual of the other species. This means that individuals at the centre of

the flock here receive less harm from the competition. On the contrary, in the classic model, individuals of the two populations are mixed together, so that the whole populations are harmed by the competition.

5.2 Conclusions

We have presented four models for non-classical population interactions, in that the populations involved in some way exhibit a socialized way of living. This investigation completes the one undertaken in [1], in that all the situations that are possible in terms of individualistic or gathering populations behavior are now analysed. The models missing in [1] are presented here: we allow predators to hunt in packs, as well as both intermingling populations to gather together, in the two cases of symbiosis and competition, so that they interact not on an individualistic basis, but rather is some coordinate fashion.

The newly introduced symbiotic model on a qualitative basis behaves like the classical one. The populations settle always at the coexistence equilibrium. Only, their levels are quantitatively smaller than in the classical case since the mutually beneficial interactions in the new model are somewhat reduced.

For predator-prey interactions in the presence of predators' pack hunting, we may have the prey behave in herds or individualistically. The most prominent discrepancy between these two cases is the fact that both populations may disappear, under specific unfortunate conditions, when the prey use a defensive coordinate strategy. This does not happen instead if they move loose in the environment, i.e. exhibit individualistic behavior, since they attain a coexistence equilibrium. This finding is quite counterintuitive, because it could imply that the defensive mechanism is ineffective. But an interpretation could be provided, since herds are more easily encountered by predators in their wanderings than individuals who can more easily hide in the terrain configuration. Once the prey herds are completely wiped out, the predators also will disappear, since they are assumed not to be generalist, i.e. their only food source is the prey under consideration. Ecosystem extinction has also been rarely observed in the model without pack predation, [33]. The system with prey herd behavior also shows limit cycles, i.e. the populations can coexist also through persistent oscillations, not only at a stable equilibrium, which instead is the only possible system's outcome for the model with individualistic prey. A similar result had been discovered earlier in case of individualistic predators hunting, [1], constituting the major difference between the prey group defense model with uncoordinated predation and the classical predator-prey system. Finally, on the quantitative side, the coexistence population values for these two models with pack hunting differ, but without specific informations on the parameter values it is not possible to assess which system will provide higher population values.

The competition system presented here allows again the extinction of both populations, under unfavorable circumstances, while this never happens for the classical model. Ecosystem disappearance occurs when (4.2) holds, a condition that in the nondimensional model is equivalent to

$$a > bc, \tag{5.1}$$

as stated in Proposition 15. When the competition system thrives, it does at higher levels for both

populations than those achieved in the classical model. Thus in this case populations coordinated behavior boosts their respective sizes, in case the system parameters are in the range for which coexistence occurs.

But the major finding in this context of social behavior among all possible populations behavior is found for the competition case. Indeed the system in suitable conditions can show the phenomenon of competitive exclusion as the classical model does, but in addition we have discovered that both populations can thrive, together with the situations predicted by the competitive exclusion principle. In other words, we have found that the rather simple model (4.1) (or in nondimensional form (A.8)) may exhibit tristability, see once more the right picture in Figure 3. This appears to be a novel and quite interesting finding further characterizing the systems with socialized behaviors. The authors do not know of any other simple related model with such behavior.

Acknowledgment: The research has been partially supported by the project "Metodi numerici nelle scienze applicate" of the Dipartimento di Matematica "Giuseppe Peano". The authors thank the referees for their constructive criticism, that helped in reshaping the paper for a better presentation of the results.

References

[1] V. Ajraldi, M. Pittavino, E. Venturino, *Modeling herd behavior in population systems*, Nonlinear Analysis: Real World Applications, 12 (2011) 2319-2338.

[2] M. Banerjee, B. W. Kooi, E. Venturino, *An ecoepidemic model with prey herd behavior and predator feeding saturation response on both healthy and diseased prey*, Mathematical Models in Natural Phenomena, 12 (2), 133–161, 2017; https://doi.org/10.1051/mmnp/201712208

[3] P.A. Braza, *Predator prey dynamics with square root functional responses*, Nonlinear Analysis: Real World Applications, 13 (2012) 1837-1843.

[4] S. P. Bera, A. Maiti, and G. P. Samanta, *Stochastic analysis of a prey-predator model with herd behaviour of prey*, Nonlinear Analysis: Modelling and Control, 21 (3) (2016) 345-361.

[5] S. P. Bera, A. Maiti, and G. P. Samanta, *Dynamics of a food chain model with herd behaviour of the prey*, Model. Earth Syst. Environ., 2(131) (2016) DOI 10.1007/s40808-016-0189-4.

[6] I. M. Bulai, E. Venturino, *Shape effects on herd behavior in ecological interacting population models*, Mathematics and Computers in Simulation, 2017. https://doi.org/10.1016/j.matcom.2017.04.009

[7] E. Caccherano, S. Chatterjee, L. Costa Giani, L. Il Grande, T. Romano, G. Visconti, E. Venturino, *Models of symbiotic associations in food chains*, in Symbiosis: Evolution, Biology and Ecological Effects, A.F. Camisão and C.C. Pedroso (Editors), Nova Science Publishers, Hauppauge, NY, 189-234, 2012.

[8] E. Cagliero, E. Venturino, *Ecoepidemics with infected prey in herd defense: the harmless and toxic cases*, IJCM, 93(1), 108-127, 2016. doi: 10.1080/00207160.2014.988614. doi: 10.1080/00207160.2014.988614.

[9] R. Cavoretto, A. De Rossi, E. Perracchione, E. Venturino, *Reconstruction of separatrix curves and surfaces in squirrels competition models with niche*, Proceedings of the 2013 International Conference on Computational and Mathematical Methods in Science and Engineering, I.P. Hamilton, J. Vigo-Aguiar, H. Hadeli, P. Alonso, M.T. De Bustos, M. Demiralp, J.A. Ferreira, A.Q.M. Khaliq, J.a. López-Ramos, P. Oliveira, J.C. Reboredo, M. Van Daele, E. Venturino, J. Whiteman, B. Wade (Editors) Almeria, Spain, June 24th-27th, 2013, v. 3, p. 400-411.

[10] R. Cavoretto, A. De Rossi, E. Perracchione, E. Venturino, *Reliable approximation of separatrix manifolds in competition models with safety niches*, International Journal of Computer Mathematics, 92(9), 1826-1837 (2015). http://dx.doi.org/10.1080/00207160.2013.867955

[11] R. Cavoretto, A. De Rossi, E. Perracchione, E. Venturino, *Robust approximation algorithms for the detection of attraction basins in dynamical systems*, to appear in Journal of Scientific Computing

[12] C. Cosner, D.L. DeAngelis, J.S. Ault, D.B. Olson, *Effects of Spatial Grouping on the Functional Response of Predators*, Theoretical Population Biology, 56, (1999) 65-75.

[13] E. Francomano, F. M. Hilker, M. Paliaga, E. Venturino, *On basins of attraction for a predator-prey model via meshless approximation*, to appear in AIP NUMTA 2016.

[14] E. Francomano, F. M. Hilker, M. Paliaga, E. Venturino, *An efficient method to reconstruct invariant manifolds of saddle points*, to appear in DRNA

[15] H.I. Freedman, G. Wolkowicz, *Predator-prey systems with group defence: the paradox of enrichment revisited*, Bull. Math. Biol., 48 (1986) 493-508.

[16] S.A.H. Geritz, M. Gyllenberg, *Group defence and the predator's functional response*, Journal of Mathematical Biology 66, (2013) 705-717.

[17] I. Giardina, *Collective behavior in animal groups: theoretical models and empirical studies*, HFSP J. 2008 August; 2(4): 205-219, doi: 10.2976/1.2961038.

[18] G. Gimmelli, B. W. Kooi, E. Venturino, *Ecoepidemic models with prey group defense and feeding saturation*, Ecological Complexity, 22 (2015) 50-58.

[19] M. Haque, E. Venturino, *Mathematical models of diseases spreading in symbiotic communities*, in J.D. Harris, P.L. Brown (Editors), Wildlife: Destruction, Conservation and Biodiversity, NOVA Science Publishers, New York, 2009, 135-179.

[20] M. J. Harrison, *Signaling in the arbuscular mycorrhizal symbiosis*, Annu. Rev. Microbiol., 59: 19–42, 2005. doi:10.1146/annurev.micro.58.030603.123749, PMID 16153162

[21] M. P. Hassell, G. C. Varley, *New inductive population model for insect parasites and its bearing on biological control*, Nature (London) 223 (1969) 1133-1137.

[22] B.W. Kooi, E. Venturino, *Ecoepidemic predator-prey model with feeding satiation, prey herd behavior and abandoned infected prey*, Math. Biosc, 274 (2016) 58-72.

[23] A. Maiti, P. Sen, D. Manna, and G.P. Samanta, *A predator-prey system with herd behaviour and strong Allee effect*, Nonlinear Dynamics and Systems Theory, 16(1) (2016) 86-101.

[24] H. Malchow, S. Petrovskii, E. Venturino, *Spatiotemporal patterns in Ecology and Epidemiology*, CRC, Boca Raton, 2008.

[25] F. Mavrot, F. Zimmermann, E.M. Vilei, M.P. Ryser-Degiorgis, *Is the development of infectious keratoconjunctivitis in Alpine ibex and Alpine chamois influenced by topographic features?*, European Journal of Wildlife Research, 58(5), 869-874, 2012.

[26] P. Nardon, H. Charles, *"Morphological aspects of symbiosis", Symbiosis: Mechanisms and Systems*. Dordercht/boson/London, Kluwer Academic Publishers, 4: 15–44, 2002. doi:10.1007/0-306-48173-1_2

[27] S. Paracer, V. Ahmadjian, *Symbiosis: An Introduction to Biological Associations*, Oxford [Oxfordshire]: Oxford University Press, 2000. ISBN 0-19-511806-5

[28] L. Perko, *Differential Equations and Dynamical Systems*, Springer, New York, 2000.

[29] J. Sapp, *Evolution by association: a history of symbiosis*, Oxford [Oxfordshire]: Oxford University Press, 1994. ISBN 0-19-508821-2

[30] A. Schüssler, D. Schwarzott, C. Walker, *A new fungal phylum, the Glomeromycota: phylogeny and evolution*, Mycol. Res., 105 (12): 1413-1421, 2001. doi:10.1017/S0953756201005196

[31] D.J.T Sumpter, *The principles of collective animal behaviour*, Phil. Trans. R. Soc. B 29, v. 361, n. 1465 (2006) 5-22, doi: 10.1098/rstb.2005.1733

[32] R.K. Trench, J.E. Boyle and D.C. Smith, *The Association between Chloroplasts of Codium fragile and the Mollusc Elysia viridis. I. Characteristics of isolated Codium chloroplasts*, Proceedings of the Royal Society of London. Series B, Biological Sciences 184 (1074): 51–61, 1973. doi:10.1098/rspb.1973.0030.

[33] E. Venturino, S. Petrovskii, *Spatiotemporal Behavior of a Prey-Predator System with a Group Defense for Prey*, Ecological Complexity, 14 (2013) 37-47.

[34] P. Waltman, *Competition Models in Population Biology*, SIAM CBMS-NSF Regional Conference Series in Applied Mathematics, Philadelphia, 1983.

Appendix

.1

A0 - Preliminary results

A0.1 - Extinction in finite time

Proposition 1. *The system (2.2) admits trajectories for which the prey go to extinction in finite time, if their initial conditions lie in the set (2.8).*

Proof. We follow with suitable modifications the argument exposed in [33]. From the second equation in (2.2) we get the differential inequality

$$\frac{dP}{dt} \geq -mP \tag{A.1}$$

from which $P(t) \geq \widehat{P}(t) = P_0 \exp(-mt)$, where the function $\widehat{P}(t)$ denotes the solution of the differential equation corresponding to (A.1), with $\widehat{P}(0) = P(0)$. From the first equation in (2.2) we have further

$$\frac{dQ}{dt} \leq rQ - q\sqrt{P}\sqrt{Q} \leq rQ - q\sqrt{\widehat{P}}\sqrt{Q}. \tag{A.2}$$

Let $\widehat{Q}(t)$ denote the solution of the differential equation obtained from (A.2) using the rightmost term, with $\widehat{Q}(0) = Q(0)$. It follows that $Q(t) \leq \widehat{Q}(t)$. Using the integrating factor $W(t) = \widehat{Q}(t)\exp(-rt)$, we obtain

$$\sqrt{W(t)} = \sqrt{W(0)} - \frac{q\sqrt{P(0)}}{m+r}h(t), \quad h(t) = \left[1 - \exp\left(-\frac{m+r}{2}t\right)\right], \tag{A.3}$$

with finite extinction time t^* obtained by setting $W(t^*) = 0$, observing that $W(0) = \widehat{Q}(0) = Q(0)$:

$$t^* = -\frac{2}{m+r}\ln\left(1 - \frac{m+r}{q}\sqrt{\frac{Q(0)}{P(0)}}\right).$$

The function $h(t)$ in (A.3) is an increasing function of t with $h(0) = 0$, $h(\infty) = 1$, so that there is a t^* for which $W(t^*) = \widehat{Q}(t^*) = 0$ if and only if

$$\sqrt{W(0)} < \frac{q\sqrt{P(0)}}{m+r}. \tag{A.4}$$

Since $W(0) = Q(0)$, we have $\widehat{Q}(t^*) = 0$ if the following inequality for the initial conditions of the trajectories is satisfied,

$$\sqrt{P(0)} > \frac{m+r}{q}\sqrt{W(0)},$$

from which the set Ξ given in (2.8) is immediately obtained. □

A0.2 - Models simplification

As remarked in [1], singularities could arise in the system's Jacobian when one or both populations vanish. This may cause difficulties in the analysis, so that we reformulate the model to avoid them.

For the predator-prey cases rescaling for the model (2.1) is obtained through

$$X = \frac{Q}{K}, \qquad Y = \frac{q\sqrt{P}}{m}, \qquad \tau = mt,$$

and defining the new parameters

$$b = \frac{r}{m}, \qquad c = \frac{pqK}{2m^2}.$$

The adimensionalized system for the pack predation–individual prey model can thus be written as

$$\frac{dX}{d\tau} = b\,(1-X)\,X - XY, \quad \frac{dY}{d\tau} = -\frac{1}{2}Y + cX, \tag{A.5}$$

while in the absence of predators, the system reduces just to the first equation. In this case, easily, the prey follow a logistic growth, toward the adimensionalized carrying capacity $X_1 = 1$.

For (2.2) we have instead

$$X = \sqrt{\frac{Q}{K}}, \qquad Y = \frac{q}{2m}\sqrt{\frac{P}{K}}, \qquad \tau = mt.$$

Define now the adimensionalized parameters

$$e = \frac{r}{2m}, \qquad f = \frac{pq}{4m^2}.$$

The adimensionalized system for $Y > 0$ for the pack predation–prey herd ecosystem becomes finally

$$\frac{dX}{d\tau} = e(1-X^2)X - Y, \quad \frac{dY}{d\tau} = -\frac{1}{2}Y + fX. \tag{A.6}$$

For both models (3.1) and (4.1) we instead define new variables as follows

$$X(\tau) = \sqrt{\frac{Q(t)}{K_Q}}, \;\; Y(\tau) = \sqrt{\frac{P(t)}{K_P}}, \;\; \tau = t\frac{q\sqrt{K_P}}{2\sqrt{K_Q}},$$

as well as new adimensionalized parameters

$$a = \frac{K_Q}{K_P}\frac{p}{q}, \;\; b = \frac{r\sqrt{K_Q}}{q\sqrt{K_P}}, \;\; c = \frac{m\sqrt{K_Q}}{q\sqrt{K_P}}.$$

The adimensionalized systems read, for the symbiotic case (3.1)

$$\frac{dX}{d\tau} = b(1-X^2)X + Y, \quad \frac{dY}{d\tau} = c(1-Y^2)Y + aX, \tag{A.7}$$

while for the competing situation (4.1) we find

$$\frac{dX}{d\tau} = b(1-X^2)X - Y, \quad \frac{dY}{d\tau} = c(1-Y^2)Y - aX. \tag{A.8}$$

All the new adimensionalized parameters are combinations of the old nonnegative parameters r, m, p, q, K; as a consequence, they must be nonnegative as well.

Remark 2. *Note that these reformulated group behavior models need a special care in treating vanishing populations, because in eliminating the singularity we divide by X and Y, except for X in the case (A.5). Therefore all the simplified models (A.7)-(A.6) hold for strictly positive populations. If one population vanishes, no information can be gathered by the latter, we rather have to turn to the original formulations (3.1)-(4.1).*

For the later analysis of the equilibria stability it is imperative to consider the Jacobians of these systems. We find the following matrices respectively, for the predator-prey cases, the Jacobian of (A.5) is

$$J^{PP1} \equiv \begin{pmatrix} b-2bX-Y & -X \\ c & -\frac{1}{2} \end{pmatrix}, \tag{A.9}$$

while the one for (A.6) reads

$$J^{PP2} \equiv \begin{pmatrix} e(1-3X^2) & -1 \\ f & -\frac{1}{2} \end{pmatrix}. \tag{A.10}$$

Considering the symbiotic and competing situations, for (A.7) we find

$$J^{S} \equiv \begin{pmatrix} b(1-3X^2) & 1 \\ a & c(1-3Y^2) \end{pmatrix} \tag{A.11}$$

and for (A.8) we have

$$J^{C} \equiv \begin{pmatrix} b(1-3X^2) & -1 \\ -a & c(1-3Y^2) \end{pmatrix}. \tag{A.12}$$

A1 - Analysis of predator-prey ecosystems

A1.1 - Pack predation and individualistic prey behavior

Proposition 3. *All positive solutions of the pack predation-individual prey system (A.5) are forward bounded.*

Proof. Introducing the environment total population, $Z(\tau) = X(\tau) + Y(\tau)$ and summing the equations in (A.5), we have

$$\frac{dZ}{d\tau} = -\frac{1}{2}Y + cX + bX - bX^2 - XY = -\frac{1}{2}Z + \left(c + b + \frac{1}{2} - bX - Y\right)X.$$

Take the maximum of the parabola in X on the right hand side, to obtain

$$\frac{dZ}{d\tau}+\frac{1}{2}Z\leq\left(c+b+\frac{1}{2}-bX\right)X\leq\frac{\left(c+b+\frac{1}{2}\right)^2}{4b}\equiv\bar{M}.$$

The above differential inequality leads to

$$Z(\tau)\leq Z(0)e^{-\frac{1}{2}\tau}+2\bar{M}\left(1-e^{-\frac{1}{2}\tau}\right)\leq\max\left\{Z(0),\bar{M}\right\}=M.$$

Note that the positive quadrant is positively invariant for (A.5). Indeed, the open positive Y axis is an orbit of system (A.5), thus it cannot be crossed by other system trajectories. The axis $Y=0$ from the second equation instead repels trajectories. Because the total population is forward bounded, and in view of the fact that the positive quadrant is positively invariant, also each individual population X and Y is forward bounded as well. □

Proposition 4. *The coexistence equilibrium $E_2^{[pi]}$ (2.4) of the system (2.1) is always locally asymptotically stable.*

Proof. If J_2^{PP1} denotes the Jacobian matrix (A.9) evaluated at $E_2^{[pi]}$, the Routh-Hurwitz criterion gives

$$\det(J_2^{PP1})=-\frac{1}{2}b+\frac{b^2+2bc}{b+2c}=\frac{1}{2}b>0,\quad \text{tr}(J_2^{PP1})=-\frac{1}{2}+b-\frac{2b^2+2bc}{b+2c}=-\frac{2b^2+2c+b}{2(b+2c)}<0. \tag{A.13}$$

Both conditions hold so that the eigenvalues have negative real part and $E_2^{[pi]}$ is always a stable equilibrium. □

Remark 5. *For (A.5) Hopf bifurcations cannot arise at coexistence, since in (A.13) tr$(J_2^{PP1})<0$ is a strict inequality.*

Proposition 6. *The coexistence equilibrium $E_2^{[pi]}$ of the pack predation-individual prey system (A.5) is also globally asymptotically stable in the open positive quadrant.*

Proof. We know already that the open positive quadrant is positively invariant and the solutions are forward bounded. Note further that by Dulac's criterion, no limit cycles can arise. Take indeed $g(X,Y)=(XY)^{-1}$, to get

$$\begin{aligned}\frac{\partial}{\partial X}\left[g(X,Y)\frac{dX}{d\tau}\right]+\frac{\partial}{\partial Y}\left[g(X,Y)\frac{dY}{d\tau}\right]&=\frac{\partial}{\partial X}\left[b(1-X)\frac{1}{Y}-1\right]+\frac{\partial}{\partial Y}\left[-\frac{1}{2X}+\frac{c}{Y}\right]\\&=-\frac{b}{Y}-\frac{c}{Y^2}<0.\end{aligned}$$

By the Poincaré-Bendixson theorem, global stability follows. □

The phase plane picture also supports these conclusions as well, Figure 7.

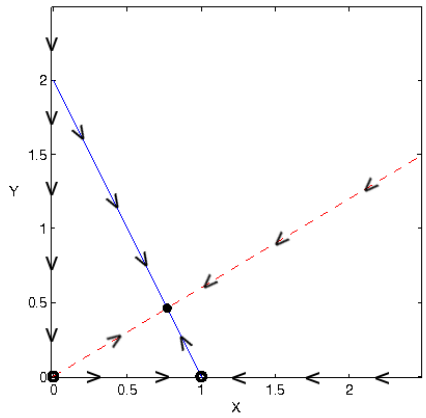

Figure 7: Phase plane sketch of the model (2.1) with parameters values $b = 2$, $c = 0.3$, corresponding to the original parameter values $r = 0.6$, $m = 0.3$, $p = 0.0072$, $q = 1.5$, $K = 5$. Blue continuous line: population X nullcline; red dashed line: population Y nullcline.

A1.2 - Analysis of pack predation and prey herd behavior

Proposition 7. *All positive solutions of the pack hunting-prey herd behavior system (A.6) are forward bounded.*

Proof. First of all, for an arbitrary $k \geq 0$, we have from the first equation in (A.6):

$$\frac{dX}{d\tau} + kX \leq (e+k)X - eX^3 = \varphi(X) \leq \varphi_m, \quad \varphi_m = \varphi(X_m), \quad X_m = \sqrt{\frac{e+k}{3e}},$$

from which

$$X(\tau) \leq \max\left\{X(0), \varphi_m k^{-1}\right\} = \widetilde{X}.$$

Then from the second equation in (A.6) solving the differential inequality we obtain the estimate

$$\frac{dY}{d\tau} \leq -\frac{1}{2}Y + f\widetilde{X}, \quad Y(\tau) \leq Y(0)e^{-\frac{1}{2}\tau} + 2f\widetilde{X}(1 - e^{-\frac{1}{2}\tau}) \leq \max\left\{Y(0), 2f\widetilde{X}\right\} = \widetilde{Y}. \quad \text{(A.14)}$$

Furthermore, from the second equation (A.6) the trajectories are repelled away from the X axis. Recalling that (A.6) holds for $X \neq 0$, using (A.14) in the first equation of (A.6), we can bound X only with a possibly negative value:

$$\frac{dX}{dt} \geq -eX^3 - \widetilde{Y} \quad X(t) \geq \left(et + X(0)^{-2}\right)^{-\frac{1}{2}} - \sqrt[3]{\frac{\widetilde{Y}}{3}}.$$

In this case, as discussed in Remark 1, if X drops to the value 0, (A.6) is not valid and we need to return to the original formulation (2.2). But for the latter as remarked in [33], on the Y axis the differential system does not satisfy the Lipschitz condition, so that uniqueness of the solutions

is lost. Technically, there are solutions that drift into the negative X half plane. We need to understand that they are not biological, and replace them by trajectories moving downwards along the Y axis to the origin. The ecosystem collapses in finite time, as also remarked in [18, 22, 2]. □

In view of the fact that the ecosystem may disappear in finite time, [18, 22, 2], recall also the set Ξ given in (2.8), we investigate the stability of the origin in (A.6) as well.

Proposition 8. *The origin $\widehat{E}_0$ and coexistence $\widehat{E}_2^{[ph]}$ are the equilibria of the pack hunting-prey herd behavior system (A.6), with population values and feasibility condition given by*

$$\widehat{E}_2^{[ph]} = \left(\widehat{X}_2^{[ph]}, \widehat{Y}_2^{[ph]}\right), \quad \widehat{X}_2^{[ph]} = \sqrt{1 - 2\frac{f}{e}}, \quad \widehat{Y}_2^{[ph]} = 2f\widehat{X}_2^{[ph]}; \quad e \geq 2f. \tag{A.15}$$

There is a transcritical bifurcation with $\widehat{E}_2^{[ph]}$ emanating from $\widehat{E}_0$ when the parameter e raises up to attain the critical value $e^* = 2f$.

Proof. The first part of the statement is easy. The characteristic polynomial at the origin $\widehat{E}_0$ is

$$\lambda^2 + \left(\frac{1}{2} - e\right)\lambda + f - \frac{1}{2}e = 0.$$

The Routh-Hurwitz stability conditions for the origin $\widehat{E}_0$ then become

$$2f > e, \qquad e < \frac{1}{2}. \tag{A.16}$$

The second claim follows comparing the first inequality in (A.16) with the feasibility condition in (A.15). In fact, at e^* the origin becomes unstable, while instead $\widehat{E}_2^{[ph]}$ becomes feasible. □

Proposition 9. *For the pack hunting-prey herd behavior system (A.6), the equilibrium $\widehat{E}_0$ when locally asymptotically stable, namely the conditions (A.16) hold, is also globally asymptotically stable in the open positive quadrant.*

Proof. Since the open positive quadrant is positively invariant and the solutions there forward bounded, using Dulac's criterion as follows, the existence of cycles is ruled out. This time take $g(X, Y) = 1$, to get in this case

$$\begin{aligned}\frac{\partial}{\partial X}\left[g(X,Y)\frac{dX}{d\tau}\right] + \frac{\partial}{\partial Y}\left[g(X,Y)\frac{dY}{d\tau}\right] &= \frac{\partial}{\partial X}\left[e(1-X^2)X - Y\right] + \frac{\partial}{\partial Y}\left[-\frac{1}{2}Y + fX\right] \\ &= e - 3eX^2 - \frac{1}{2} < 0,\end{aligned}$$

in view of the second local stability condition of the origin, (A.16). $\widehat{E}_0$ must also be globally asymptotically stable by the Poincaré-Bendixson theorem. □

Proposition 10. *The coexistence equilibrium $\widehat{E}_2^{[ph]}$ of the system (A.6) is a locally asymptotically stable equilibrium if*

$$tr(\widehat{J}_2^{PP2}) = -2e + 6f - \frac{1}{2} < 0. \tag{A.17}$$

If $e > \max\left\{\frac{1}{2}, 3f - \frac{1}{4}\right\}$ (A.17) holds. But if $2f < e < 3f - \frac{1}{4}$ (A.17) is not true and $\widehat{E}_2^{[ph]}$ is unstable.

Proof. Let the Jacobian evaluated at $\widehat{E}_2^{[ph]}$ be denoted by $\widehat{J}_2^{PP2}$. The Routh-Hurwitz conditions are now $\det(J_2^{PP2}) = e - 2f > 0$, which always holds if the feasibility condition (A.15) is strictly satisfied, and (A.17). If the latter holds then $\widehat{E}_2^{[ph]}$ is stable. □

Figures 8 and 9 illustrate geometrically the two situations in which $\widehat{E}_2^{[ph]}$ is feasible and when it is unfeasible. The different possible ecosystem outcomes in the parameter space, corresponding to the various situations of (A.17), are shown in Figure 10.

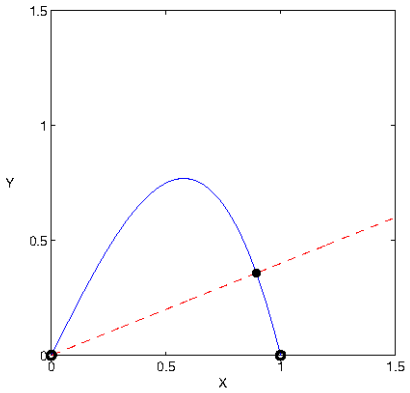

Figure 8: Nullclines of system (A.6) with $e \geq 2f$, both $\widehat{E}_0$ and $\widehat{E}_2^{[ph]}$ exist. Parameter values: $e = 2$, $f = 0.2$, $r = 0.5$, $m = 0.125$, $p = 0.5$, $q = 0.025$, $K = 10$. Blue continuous line: population X nullcline; red dashed line: population Y nullcline. The full dot indicates the stable equilibrium $\widehat{E}_2^{[ph]}$.

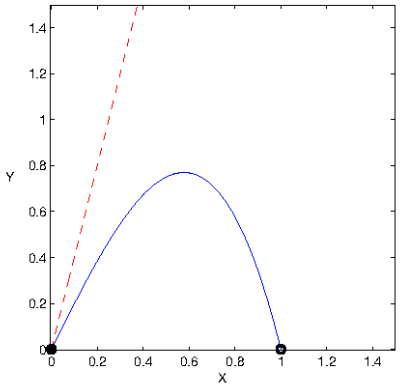

Figure 9: Nullclines of system (A.6) with $e < 2f$, $\widehat{E}_2^{[ph]}$ is unfeasible. Parameter values: $e = 2$, $f = 2.0$, $r = 0.5$, $m = 0.125$, $p = 0.5$, $q = 0.25$, $K = 10$. Blue continuous line: population X nullcline; red dashed line: population Y nullcline. The full dot indicates the stable equilibrium $\widehat{E}_0$.

Proposition 11. *The the pack hunting-prey herd behavior system (A.6) admits a Hopf bifurcation at the coexistence equilibrium $\widehat{E}_2^{[ph]}$ when the bifurcation parameter e crosses the critical value $e^\dagger$ that corresponds to $r^\dagger$ given in (2.7).*

$$e^\dagger = 3f - \frac{1}{4}. \tag{A.18}$$

Proof. In addition to the transcritical bifurcation of Proposition 8, we show now that special parameters combinations originate Hopf bifurcations near $\widehat{E}_2^{[ph]}$. Recall that purely imaginary eigenvalues are needed, and this occurs when the trace of the Jacobian vanishes. Thus (A.17) must become an equality and the constant term in the characteristic equation is positive, $\det(\widehat{J}_2^{PP2}) = e - 2f > 0$. But the latter holds from (A.15). □

Thus the solutions of the system start oscillating in a persistent manner around the coexistence equilibrium when the bifurcation parameter e crosses the critical value $e^{\dagger}$, (A.18). This result is observed in Figure 10, where the thick straight line indicates the critical parameter values.

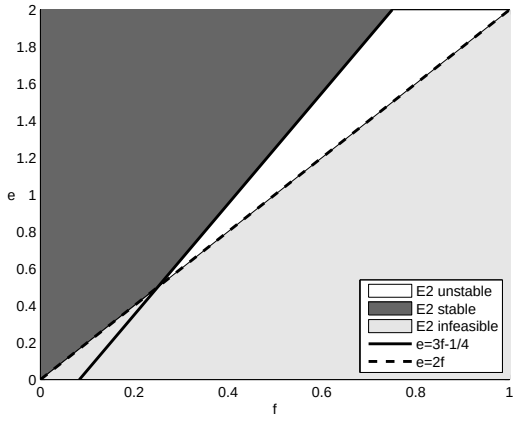

Figure 10: Region of the $f - e$ parameter space in which the coexistence equilibrium of (A.6) is stable.

A3 - Analysis of the symbiotic model

The classical case

The results of the classical case,

$$\frac{dQ}{dt} = r\left(1 - \frac{Q}{K_Q}\right)Q + qPQ, \quad \frac{dP}{dt} = m\left(1 - \frac{P}{K_P}\right)P + pPQ, \tag{A.19}$$

are summarized in [1]. Extensions of classical symbiotic systems have been recently investigated, to models incorporating diseases [19], or to food chains, [7]. In short, the three equilibria in which at least one population vanishes are unstable, $\widehat{E_0^S} = (0, 0)$, $\widehat{E_1^S} = (K_Q, 0)$ and $\widehat{E_2^S} = (0, K_P)$. The coexistence equilibrium

$$\widehat{E_3^S} = \left(\frac{K_Q m(r + pK_P)}{rm - pqK_P K_Q}, \frac{K_P r(m + qK_Q)}{rm - pqK_P K_Q}\right)$$

is unconditionally stable when feasible, i.e. $rm < pqK_PK_Q$. Note that if $\widehat{E_3^S}$ is unfeasible the trajectories are unbounded, which is biologically scarcely possible in view of the environment's limited resources.

The herd behavior case

Looking for the coexistence equilibria, solving for Y the first equation in (A.7) and substituting into the second one, we are led to the ninth degree equation

$$X[a - bc(1 - X^2)(1 - b^2X^6 + 2b^2X^4 - b^2X^2)] = 0.$$

Factoring out X, the remaining equation is a quartic in X^2, but still with cumbersome analytic solutions. However, we can turn to a graphical analysis of the system of equations originated by (A.7). The coexistence equilibrium will be the intersection of the two cubic functions,

$$Y_s(X) = bX(X^2 - 1), \quad X_s(Y) = \frac{c}{a}Y(Y^2 - 1), \tag{A.20}$$

obtained from the equilibrium equations of (A.7).

Proposition 12. *The coexistence equilibrium of the symbiotic system (A.7) is unique and always feasible.*

Proof. The two cubic functions (A.20) intersect the axes corresponding to their domains at three fixed points, 0 and ± 1. Further, from the largest positive root, they raise up to infinity. Since their domains are on orthogonal axes, it follows that there always exists a unique positive equilibrium. □

A typical situation is shown in Figure 11 for a choice of hypothetical parameter values. Note that in this case, there are nine intersections among the two curves Y_s and X_s. For other situations, some of the intersections in the second and fourth quadrant may disappear. But the origin and the ones in the first and third quadrants exist always. The intersection in the first quadrant is feasible, leading to the coexistence equilibrium $E_3^S = (X_3^S, Y_3^S)$. The positive solutions of (A.7) are forward bounded, as can easily be seen by drawing the system's trajectories, a claim that is also mathematically rigorously proven in Proposition 14 below.

Proposition 13. *No Hopf bifurcations can arise at the coexistence equilibrium of the symbiotic system (A.7).*

Proof. To have Hopf bifurcations, we need purely imaginary eigenvalues. This occurs when the trace of the Jacobian vanishes and simultaneously the determinant is positive, i.e.

$$b(1 - 3X^2) + c(1 - 3Y^2) = 0, \quad b(1 - 3X^2)c(1 - 3Y^2) - a > 0. \tag{A.21}$$

It can be easily seen that solving for b from the first condition and substituting into the second one, we find

$$a < -c^2(1 - 3Y^2)^2 < 0,$$

which is a contradiction. □

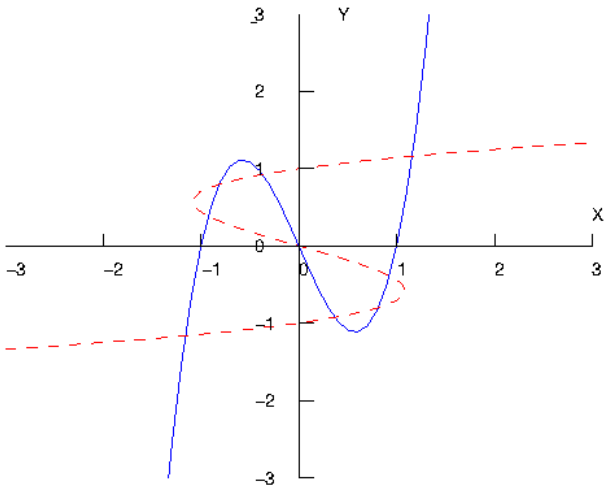

Figure 11: Nullclines of equations system from (A.7). The X nullcline corresponds to the blue continuous curve $Y = Y_s(X)$, conversely The Y nullcline corresponds to the red dashed function $X = X_s(Y)$. The phase plane of interest is obviously only the set $\{(X, Y) : X \geq 0, Y \geq 0\}$. The figure is obtained for the following parameter values $a = 0.6$, $b = 2.9$, $c = 1.7$, $r = 2.9$, $m = 1.7$, $p = 0.6$, $q = 1$, $K_P = 10$, $K_Q = 10$.

Proposition 14. *The positive solutions of (A.7) are forward bounded. Its coexistence equilibrium E_3^S is globally asympotically stable.*

Proof. We follow the outline of [1]. It is enough to take a large enough box B in the first quadrant that contains the coexistence equilibrium.

On the vertical and on the horizontal sides we show that the dynamical system's flow enters into the box. Indeed, take a point $\widehat{U} = (\widehat{X}, \widehat{Y})$ in the phase plane, with $\widehat{X} > X_3^S$, $\widehat{Y} > Y_3^S$ and lying below the isocline $X' = 0$ and above the isocline $Y' = 0$, thus for which the inequalities $X < X_s$ and $Y < Y_s$ hold. It identifies the rectangle B in the phase plane, with opposite vertex given by the origin, which is a positively invariant set for the model (A.7). In fact on its vertical side $Y = \widehat{Y}$ we have $Y' < 0$ while instead $X' < 0$ on the horizontal line $X = \widehat{X}$, showing that the flow of (A.7) enters into B on these sides.

The axes cannot be crossed, on biological grounds, and mathematically, because both axes indeed repel the trajectories. Note that in the original situation, however, the square root singularity in (3.1) prevents the right hand side of the dynamical system to be Lipschitz continuous when the corresponding population vanishes, so that the assumption for the uniqueness theorem fails on the axes. But as mentioned in the model formulation, we understand that the differential equations hold only in the interior of the first quadrant, on the coordinate axes they are replaced by corresponding equations in which the vanishing population is removed and whose behavior has already been discussed, leading to equilibria on these axes, either the carrying capacities or the origin.

Thus B is a positively invariant set, from which the first claim follows. By the Poincaré-

Bendixson theorem, since there are no limit cycles by Proposition 13, the coexistence equilibrium must be globally asymptotically stable. □

A4 - Analysis of the competition model

5.2.1 The classical competition model

The classical competition model,

$$\frac{dQ}{dt} = r\left(1 - \frac{Q}{K_Q}\right)Q - qPQ, \quad \frac{dP}{dt} = m\left(1 - \frac{P}{K_P}\right)P - pPQ, \tag{A.22}$$

shows under suitable circumstances the competitive exclusion principle. Thus, only one population survives, while the other one is wiped out. The system's outcome depends only on its initial conditions, so that if the system has population values lying in the attracting set of one of the equilibria, the dynamics will be drawn to it unless the environmental conditions, i.e. the parameters in the model, abruptely change.

5.2.2 The herds competition system

Although the coexistence equilibria of the competition ecosystem (A.8) could be written as the roots of the following quartic equation in X^2,

$$cb^3X^8 - 3cb^3X^6 + 3cb^3X^4 - cb(b^2+1)X^2 - a + cb = 0, \tag{A.23}$$

we prefer once more to address the issue by geometrical means since it gives a better interpretation, treating the problem as an intersection of cubic functions,

$$Y_{[1]}(X) = b(1-X^2)X, \quad X_{[2]}(Y) = \frac{c}{a}(1-Y^2)Y. \tag{A.24}$$

Proposition 15. *No feasible coexistence equilibria for the competing ecosystem (A.8) exist if (5.1) holds. Conversely, at least one feasible equilibrium exists, $E_3^C = (X_3^C, Y_3^C)$. Further, in such case, $b > \frac{3\sqrt{3}}{2}$ and $c > \frac{3\sqrt{3}}{2}a$ are sufficient conditions for three equilibria to exist, i.e. E_4^C, E_3^C and E_5^C, ordered for increasing values of their abscissae.*

Proof. Depending on the behavior of the cubic functions (A.24), there could be either three intersections (the origin and one each in the second and fourth quadrants) or five (the previous ones and one more in the first and third quadrants), or nine. The latter configuration is graphically shown in Figure 12. The feasible coexistence equilibria are just the intersections in the first quadrant. Note that no intersections in the first quadrant exist when the slopes at the origin of the two cubic functions (A.24) satisfy the inequality $Y'_{[1]}(0) < Y'_{[2]}(0)$, the latter denoting of course the inverse function of $X_{[2]}(Y)$. This condition, rephrased in terms of the parameters, becomes (5.1).

Thus, for $a > cb$ there is at most one real positive root, the one corresponding to the intersection in the fourth quadrant, that is however not feasible, and no intersection exists in the first quadrant, see the left frame in Figure 2. Thus no coexistence equilibrium arises.

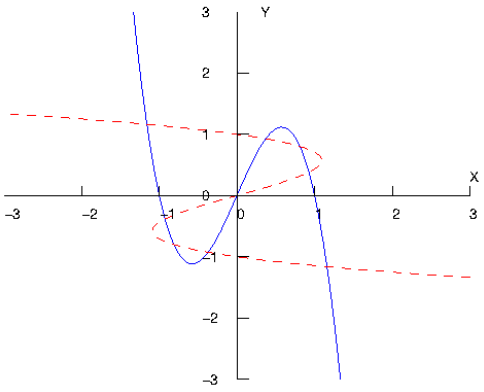

Figure 12: Graphical solution of equations system from (A.8) for the functions $Y_{[1]}(X)$ and $X_{[2]}(Y)$. Parameter values: $a = 0.6$, $b = 2.9$, $c = 1.7$, $r = 2.9$, $m = 1.7$, $p = 0.6$, $q = 1$, $K_p = 10$, $K_q = 10$. Blue continuous line: population X nullcline; red dashed line: population Y nullcline.

To better analyse the situation, we apply Descartes' rule of signs to (A.23). There are three sign variations, since the first four coefficients have alternating signs. The last one must be positive, because having already ruled out the case (5.1), we are left with $a < cb$. Descartes' rule shows that in this case there are at most 4 real positive roots. Recall that these roots correspond to the abscissae of the intersections of the curves (A.24). As discussed above we know that one positive root corresponds to the intersection that always exists in the fourth quadrant, Figure 12. This root must then be excluded. As a consequence in this case we have just one or three coexistence equilibria, see the center and right frames in Figure 2.

Sufficient conditions for three versus one equilibria to exist is that the cubic functions (A.24) have maximum Y-coordinate and X-coordinate respectively in the first quadrant greater than 1. This happens when both the following conditions hold

$$b > \frac{3\sqrt{3}}{2}, \quad c > \frac{3\sqrt{3}}{2}a.$$

□

Proposition 16. *The positive solutions of the competing system (A.8) are forward bounded.*

Proof. Observe that X decreases when $Y \leq bX(1 - X^2)$ and similarly Y decreases for $X \leq ca^{-1}Y(1 - Y^2)$. This in the phase plane corresponds to having the flow entering a suitable box Ω^C with one corner in the origin and the opposite one $\Omega^C_B = (X_B, Y_B)$ of size large enough to contain the vertices of the cubics in all cases of Figure 2. Thus we can take $X_B \geq \max\{1, X_V\}$, $Y_B \geq \max\{1, Y_V\}$, where X_V and Y_V denote respectively the relative maxima heights of the cubics. Once more, as found for the pack predation–prey herd behavior model (A.6), here both axes are not solutions of the system (A.8), but considerations along the lines of those exposed in

Proposition 8, in addition to the findings of [18, 22, 2] indicating ecosystem collapse in finite time in suitable circumstances, can be used. We omit the details. □

Proposition 17. *The coexistence equilibria of the competing system (A.8) for which either one of the conditions hold*

$$X < \frac{\sqrt{3}}{3}, \quad Y < \frac{\sqrt{3}}{3}, \tag{A.25}$$

namely E_k^C, $k = 4, 5$, are unstable.

Proof. If both (A.25) hold, the first Routh-Hurwitz condition applied to (A.12) is

$$\mathrm{tr} J^C = b(1 - 3X^2) + c(1 - 3Y^2) < 0. \tag{A.26}$$

But for the assumptions (A.25) it cannot be satisfied. If only one of (A.25) is satisfied, say the first one, from the condition on the trace we obtain $b < -c(1 - 3Y^2)(1 - 3X^2)^{-1}$ and substituting into the determinant, we have the estimate $\det J^C = b(1-3X^2)c(1-3Y^2)-a < -c^2(1-3Y^2)^2-a < 0$ so that the second Routh-Hurwitz condition is not satisfied. Hence the claim. □

Proposition 18. *The equilibrium E_3^C for which both the following conditions hold*

$$X > \frac{\sqrt{3}}{3}, \quad Y > \frac{\sqrt{3}}{3} \tag{A.27}$$

is stable.

Proof. The Routh-Hurwitz condition (A.26) easily holds. The second one applied to (A.12) requires

$$\det J^C = b(1 - 3X^2)c(1 - 3Y^2) - a > 0.$$

Observe that the slope of $Y_{[1]}(X)$ is negative at $X = 1$. Hence for the abscissa of E_3^C we must have $X_3 < 1$. Similarly $Y_3 < 1$, using the slope of $X_{[2]}(Y)$ at $Y = 1$. It follows that $b(1 - 3X^2) > -2b$, $c(1 - 3Y^2) > -2c$. Thus in turn $\det J^C > 4bc - a$. Since we are in the case $a < bc$, $\det J^C > 0$ follows. □

Remark 19. *Upon returning to the original variables, conditions (A.25) and (A.27) respectively become (4.6) and (4.7) .*

Remark 20. *There is thus a subcritical pitchfork bifurcation for which from the unstable E_3^C three equilibria arise, with the equilibrium E_3^C becoming stable and the other ones being unstable.*

Remark 21. *No Hopf bifurcations arise in this model as they do not in the symbiotic one. Using the same technique as in the proof of Proposition 14, the condition on the trace becomes an equality, so that by solving it for b we get $b = -c(1 - 3Y^2)(1 - 3X^2)^{-1}$. Substituting into the second Routh-Hurwitz condition $\det J^C > 0$, we obtain the contradiction $-c^2(1 - 3Y^2)^2 - a > 0$.*

A5 - Proof of bifurcations

For the proofs, we follow the approach and the notations of [28]. To prove that the transversality conditions are satisfied by the model (4.1) at the pitchfork and saddle-node bifurcation thresholds respectively, using the original model (4.1), the calculations cannot be performed because they need the first and second order partial derivatives of $\sqrt{P}$ and $\sqrt{Q}$ with respect to P and Q evaluated at $(0, 0)$. We therefore need to work on the suitably modified dimensionless version. For this purpose, we use the transformations

$$x(\sigma) = \sqrt{\frac{Q(t)}{K_Q}}, \quad y(\sigma) = \sqrt{\frac{P(t)}{K_P}}, \quad \sigma = t\frac{q}{2}\sqrt{\frac{K_P}{K_Q}}$$

and obtain the following transformed system

$$\frac{dx}{d\sigma} = b(1-x^2)x - y, \;\; \frac{dy}{d\sigma} = c(1-y^2)y - ax, \tag{A.28}$$

where

$$a = \frac{K_Q p}{K_P q}, \quad b = \frac{r\sqrt{K_Q}}{q\sqrt{K_P}}, \quad b = \frac{r\sqrt{K_Q}}{q\sqrt{K_P}}.$$

A5.1 - Proof of the pitchfork bifurcation

Using the parameter transformations and the parameter values $r = 0.9$, $K_Q = 10$, $q = 0.3$, $K_P = 10$, $p = 0.9$, $m_{PF} = 0.3$ we obtain $a = 3$, $b = 3$ and $c_{PF} = 1$ as the pitchfork bifurcation threshold. To verify the transversality conditions for the pitchfork bifurcation we first calculate the Jacobian matrix for the system (A.28) around $(0, 0)$ at the threshold $c_{PF} = 1$, and find

$$A = \begin{bmatrix} 3 & -1 \\ -3 & 1 \end{bmatrix}.$$

The eigenvectors corresponding to the zero eigenvalues of the matrix A and A^t are given by $v = [1, 3]^t$ and $w = [1, 1]^t$ respectively. Let$f = [f_1,\ f_2]^t$, with $f_1 = b(1-x^2)x-y$, $f_2 = c(1-y^2)y-ax$. We can now perform the following calculations:

$$f_c = \begin{bmatrix} \frac{\partial f_1}{\partial c} \\ \frac{\partial f_2}{\partial c} \end{bmatrix} = \begin{bmatrix} 0 \\ y(1-y^2) \end{bmatrix} \equiv \begin{bmatrix} F_1 \\ F_2 \end{bmatrix}, \quad Df_c = \begin{bmatrix} \frac{\partial F_1}{\partial x} & \frac{\partial F_1}{\partial y} \\ \frac{\partial F_2}{\partial x} & \frac{\partial F_2}{\partial y} \end{bmatrix} = \begin{bmatrix} 0 & 0 \\ 0 & 1-3y^2 \end{bmatrix}.$$

We further obtain

$$w^t f_c((0,0), c_{PF}) = [1,\ 1] \begin{bmatrix} 0 \\ 0 \end{bmatrix} = 0,$$

$$w^t \left[Df_c((0,0), c_{PF})v\right] = [1,\ 1] \begin{bmatrix} 0 & 0 \\ 0 & 1 \end{bmatrix} \begin{bmatrix} 1 \\ 3 \end{bmatrix} = 3 \neq 0.$$

Further,

$$\frac{\partial^2 f_1}{\partial x^2} = -6bx,\ \frac{\partial^2 f_1}{\partial x \partial y} = 0,\ \frac{\partial^2 f_1}{\partial y^2} = 0,\ \frac{\partial^2 f_2}{\partial x^2} = 0,\ \frac{\partial^2 f_2}{\partial x \partial y} = 0,\ \frac{\partial^2 f_2}{\partial y^2} = -6cy,$$

and hence

$$w^t \left[D^2 f((0,0), c_{PF})(v,v)\right] = w^t \left[\begin{array}{c} \frac{\partial^2 f_1}{\partial x^2} v_1^2 + 2\frac{\partial^2 f_1}{\partial x \partial y} v_1 v_2 + \frac{\partial^2 f_1}{\partial y^2} v_2^2 \\ \frac{\partial^2 f_2}{\partial x^2} v_1^2 + 2\frac{\partial^2 f_2}{\partial x \partial y} v_1 v_2 + \frac{\partial^2 f_2}{\partial y^2} v_2^2 \end{array} \right]_{x=0, x=0, c=c_{PF}} = 0.$$

Similarly we find

$$\begin{aligned} w^t \left[D^3 f((0,0), c_{PF})(v,v,v)\right] &= w^t \left[\begin{array}{c} \frac{\partial^3 f_1}{\partial x^3} v_1^3 + 3\frac{\partial^3 f_1}{\partial x^2 \partial y} v_1^2 v_2 + 3\frac{\partial^3 f_1}{\partial x \partial y^2} v_1 v_2^2 + \frac{\partial^3 f_1}{\partial y^3} v_2^3 \\ \frac{\partial^3 f_2}{\partial x^3} v_1^3 + 3\frac{\partial^3 f_2}{\partial x^2 \partial y} v_1^2 v_2 + 3\frac{\partial^3 f_2}{\partial x \partial y^2} v_1 v_2^2 + \frac{\partial^3 f_2}{\partial y^3} v_2^3 \end{array} \right]_{x=0, y=0, c=c_{PF}}, \\ &= [1,\ 1]^t \left[\begin{array}{c} (-18).1^3 + 3.0.1^2.3 + 3.0.1.3^2 + 0.3^3 \\ 0.1^3 + 3.0.1^2.3 + 3.0.1.3^2 + (-6).3^3 \end{array} \right] = -180 \neq 0. \end{aligned}$$

Hence the transversality conditions for the pitchfork bifurcation are satisfied.

A5.2 - Proof of the saddle-node bifurcation

For $a = 3$, $b = 3$ and $c = 6.8639$ we find an equilibrium point $E_1(0.3459, 0.9135)$ and two coincident equilibrium points $E_*(0.8767, 0.6087)$. The system (A.28) undergoes a saddle-node bifurcation at E_*. Calculating the Jacobian matrix for (A.28) at E_*, we obtain

$$B = \left[\begin{array}{cc} -3.917 & -1 \\ -3 & -0.7659 \end{array} \right].$$

The eigenvectors corresponding to the zero eigenvalues of B and B^t are given by are $[0.269,\ -1.0536]^t$ and $[0.6612,\ -0.8633]^t$ respectively.

Now we can proceed with the calculations:

$$w^t f_c(E_*, c_{SN}) = [0.6612,\ -0.8633] \left[\begin{array}{c} 0 \\ 0.3832 \end{array} \right] = -.3308 \neq 0,$$

$$\begin{aligned} w^t \left[D^2 f(E_*, c_{SN})(v,v)\right] &= \left[\begin{array}{c} 0.6612 \\ -0.8633 \end{array} \right]^t \left[\begin{array}{c} -6.3.(0.8767).(0.269)^2 + 2.0.v_1 v_2 + 0.v_2^2 \\ 0.v_1^2 + 2.0.v_1 v_2 - 6.(6.8639).(0.6087).(-1.054)^2 \end{array} \right] \\ &= 23.2681 \neq 0. \end{aligned}$$

Hence both the transversality conditions for the saddle-node bifurcation are satisfied.